Biophysical Journal
Article

Biophysical Society

Wi-Fi Live-Streaming Centrifuge Force Microscope for Benchtop Single-Molecule Experiments

Jibin Abraham Punnoose,[1] Andrew Hayden,[1] Lifeng Zhou,[1] and Ken Halvorsen[1,*]
[1]RNA Institute, SUNY at Albany, Albany, New York

ABSTRACT The ability to apply controlled forces to individual molecules has been revolutionary in shaping our understanding of biophysics in areas as diverse as dynamic bond strength, biological motor operation, and DNA replication. However, the methodology to perform single-molecule experiments remains relatively inaccessible because of cost and complexity. In 2010, we introduced the centrifuge force microscope (CFM) as a platform for accessible and high-throughput single-molecule experimentation. The CFM consists of a rotating microscope with which prescribed centrifugal forces can be applied to microsphere-tethered biomolecules. In this work, we develop and demonstrate a next-generation Wi-Fi CFM that offers unprecedented ease of use and flexibility in design. The modular CFM unit fits within a standard benchtop centrifuge and connects by Wi-Fi to an external computer for live control and streaming at near gigabit speeds. The use of commercial wireless hardware allows for flexibility in programming and provides a streamlined upgrade path as Wi-Fi technology advances. To facilitate ease of use, detailed build and setup instructions, as well as LabVIEW-based control software and MATLAB-based analysis software, are provided. We demonstrate the instrument's performance by analysis of force-dependent dissociation of short DNA duplexes of 7, 8, and 9 bp. We showcase the sensitivity of the approach by resolving distinct dissociation kinetic rates for a 7 bp duplex in which one G-C basepair is mutated to an A-T basepair.

SIGNIFICANCE The ability to apply mechanical forces to individual molecules has provided unprecedented insight into many areas of biology. Centrifugal force provides a way to increase the throughput and to decrease the cost and complexity of single-molecule experiments compared with other approaches. In this work, we show the development of a user-friendly centrifuge force microscope that enables live-streaming of high-throughput single-molecule experiments in a benchtop centrifuge. We achieved near gigabit bandwidth with standard Wi-Fi components, and we provide detailed design instructions and software to facilitate use by other labs. We demonstrate the instrument for sensitive kinetic measurements capable of resolving the difference between two DNA duplexes that differ by a single G-C to A-T substitution.

INTRODUCTION

Force-based single-molecule techniques are powerful approaches to understand complex reaction pathways and dynamic interplay of biomolecules. Techniques such as optical tweezers, magnetic tweezers, and atomic force microscopy (AFM) are the most widely used force-based single-molecule techniques and have contributed to our understanding of the influence of force on biological structures and processes (1–4). A few such examples include insight into how proteins fold (5,6), mechanisms of molecular locomotion (7), and the effect of force on the activity of biomolecules (8). These methods work by applying force to a biomolecule tethered between two surfaces via optical forces, magnetic forces, or mechanical forces (through a bending cantilever). The response of the molecule to the force is then determined by imaging the motion of one of the surfaces, typically a microsphere for optical and magnetic tweezers and a cantilever for AFM. Although the success of these methods is indisputable, they have traditionally come with some drawbacks that have limited their accessibility. The instrumentation tends to be costly (often >$100,000) and complex (e.g., laser alignment, vibration isolation, custom hardware) and typically can only probe one molecule at a time, making single-molecule biophysics (which often requires hundreds to thousands of statistics) a notoriously tedious and difficult enterprise.

The centrifuge force microscope (CFM) was conceived and developed to address these problems and became the

Submitted July 14, 2020, and accepted for publication October 8, 2020.
*Correspondence: khalvorsen@albany.edu
Editor: Thomas Perkins.
https://doi.org/10.1016/j.bpj.2020.10.017

first method to demonstrate thousands of single-molecule experiments performed in parallel (9). The primary conceptual advance of the method was the recognition that centrifugation could (in principle) be used to apply controlled, uniform, and physiologically relevant forces to many individual biomolecular tethers at once. The original thought experiment consisted of many tethered microspheres, centrifuged to generate an equal force on all microspheres simultaneously (assuming uniform size and density), applying equal tension to all of the biomolecular tethers (Fig. 1 *a*). In practice, implementing the approach came with many technical challenges inherent to microscopy-based imaging of many tethered microspheres while centrifugal force was being applied. Unlike previous spinning disk designs that used a stationary microscope (10–12), bringing our thought experiment to reality required designing and building a video microscope that could be mostly or entirely centrifuged (Fig. 1 *b*).

The first generation of CFM was intended to provide proof of concept and was considered, even among the inventors, to have a high risk of failure. The final design was a custom-built open-air centrifuge with an attached microscope unit and counterbalance (Fig. 1 *c*). An open-aperture electrical motor secured to an optical table was the core of the centrifuge. An electrical slip ring with an integrated rotary optical fiber joint enabled power and data transmission, respectively, between the rotating equipment and the stationary power electronics and computer. The first CFM achieved its goal of demonstrating proof of concept with massive multiplexing in single-molecule pulling experiments (achieving >5000 simultaneous experiments). However, the prototype had several shortcomings, including some difficulties in design, assembly, and operation, and some safety concerns that necessitated a dedicated room.

Several of these issues were solved in newer generations of CFM. In the second-generation CFM, the major development was the integration of the microscopy module into a commercial centrifuge (modified to house a rotary fiber joint) (10,11). This version increased the safety and decreased the engineering required to build a CFM while also adding new features such as built-in temperature control and push-button operation. The third-generation took the benchtop centrifuge concept further and became the first truly wireless CFM that could be used in a standard centrifuge bucket with an off-the-shelf centrifuge (12). This version further improved ease of use and accessibility to other labs. Outside of the two labs involved in the initial CFM development, a few labs have developed instruments on their own with various features. The Forde lab developed a mini-radio CFM that used wireless radio frequency transmission for a plug-and-play CFM module (13). The Hu lab developed a CFM that incorporated digital holography for three-dimensional (3D) particle tracking (14).

Whereas these implementations of the CFM have been evolving in the right direction, the current designs still face tradeoffs between complexity and performance. In a key shortcoming, our third-generation CFM was wireless and plug-and-play but lacked live streaming and real-time control. Here, we report development of our fourth-generation CFM (Fig. 1 *d*), a plug-and-play device with real-time control and data transmission over Wi-Fi. This device can be used in a commercial centrifuge without any customization and includes a user-friendly interface, making the CFM technique far more accessible to other labs. Using this next-generation CFM, we demonstrate single-molecule DNA shearing experiments that investigate the effect of force, length, and GC content on dissociation kinetics.

MATERIALS AND METHODS

Instrument design and construction

The CFM module, designed to fit within a 400-mL bucket of a commercial centrifuge (Sorvall Legend X1R; Thermo Fisher Scientific, Waltham, MA), has aspects of similarity with our previous design (12). As with our previous designs, we put emphasis on reproducibility and provide a detailed parts list, building instructions, and 3D models in the Supporting Materials and Methods and Data S1. The optical CFM components are largely unchanged from previous versions: a 40× infinity-corrected objective, turning mirrors, LED, and a diffuser. The main change in optical components was the camera, which was changed from a USB camera to a gigabit Ethernet camera (GigE) (model# BFLY-PGE-50H5M-C; FLIR Systems, Wilsonville, OR; www.flir.com;) to facilitate the Wi-Fi capabilities. The optical arrangement and housing have only minor changes and are detailed in Fig. S1.

The electrical system and the mechanical housing to mate with the centrifuge bucket were redesigned for the Wi-Fi strategy, with slightly different designs for each of the two routers we used. For power distribution, a replaceable lithium-ion battery (part# 2011; adafruit, New York, NY; www.adafruit.com) is connected to independent 5 and 12 V step-up voltage regulators (part# 2891, 2895; Pololu Robotics and Electronics, Las Vegas, NV; www.pololu.com) to power the Wi-Fi router (TL-WR902AC; TP-Link, Brea, CA; www.tp-link.com) and camera, respectively. Wiring diagrams and sketches of the instruments using two different routers are provided (Figs. S2–S5).

We assembled the required electronics, including the step-up voltage regulators for the camera and router and an LED light source on a 3D-printed housing (Fig. 1 *d*; Figs. S3 and S5; 3D files for housing are provided as Data S1). All the parts required for building the CFM are listed in Table S1.

We also have designed a counterbalance, the mass of which can be adjusted by adding or removing quarters. To maintain the center of mass, the counterbalance was designed to resemble the shape of the fully assembled CFM, printed with 40% infill with a hollow cylinder bore in the place of the lens tube, where quarters were added to fine-tune the mass. A detailed protocol for making the counterbalance is described in Supporting Materials and Methods, Note 1 (Fig. S6).

Software and networking

The housing for the CFM components and counterbalance were designed using Fusion360 2019 (www.autodesk.com). The 3D files generated for the components are given in Data S1. The 3D files were converted to printer-specific g-code using Cura v3.4.1 (ultimaker.com).

The CFM controller was written using LabVIEW 2018 (www.ni.com). The NI-IMAQdx driver in the vision acquisition module can communicate with the GigE camera, and programs can be written with built-in functions. The programs written for controlling FLIR Blackfly (catalog# BFLY-PGE-50H5M-C; FLIR Systems) with firmware version v1.42.3.00 are given in

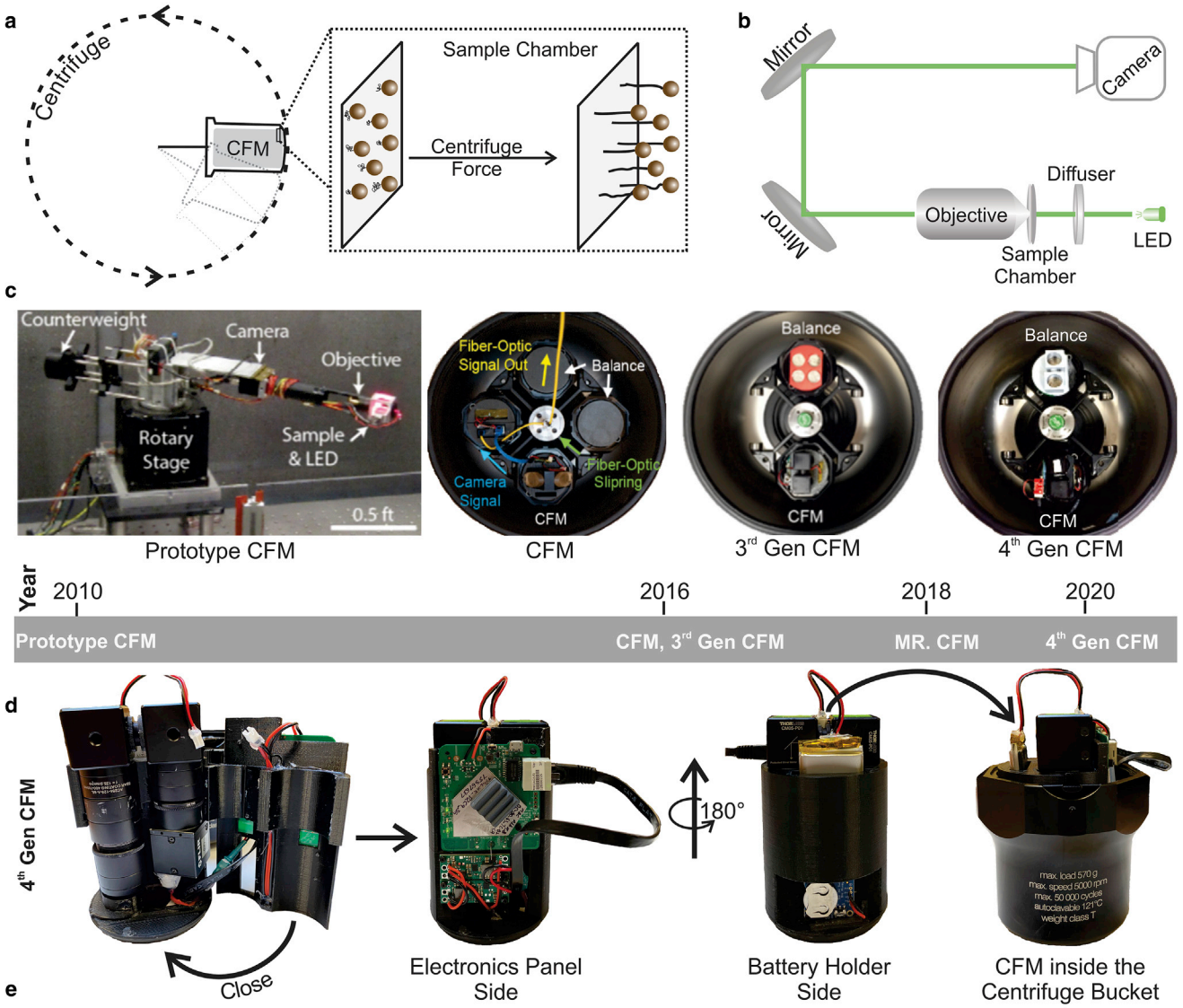

Name	Prototype CFM	CFM	3rd GenCFM	MR.CFM	4th Gen CFM
Lab	Wong Lab	Wong Lab	Halvorsen Lab	Forde Lab	Halvorsen Lab
Transmission Mode	Wired Ethernet	Wired Ethernet	Wi-Fi	Radio Signals	Wi-Fi
Transmission Rate	~800 Mb/s	~800 Mb/s	~40 Mb/s	NA	~454 Mb/s
Live Streaming & Active Control	Yes	Yes	No	Yes	Yes
Plug & Play	No	No	Yes	Yes	Yes
Centrifuge Type	Custom-made, Open air	Modified-Commercial Benchtop	Commercial Benchtop	Commercial Benchtop	Commercial Benchtop

FIGURE 1 Working principles of the centrifuge force microscope (CFM) and its evolution. (*a*) Schematics of the working principle of the CFM are shown. Force is applied to the molecule of interest tethered between a glass-slide and microscopic bead and placed inside a centrifuge. The force experienced by the sandwiched molecule is proportional to the square of the angular velocity and the size of the bead. (*b*) Schematics of the optic assembly of the CFM are shown. The tethered microsphere is visualized using a 40× or 20× infinite conjugate objective and imaged using a machine vision camera. (*c*) Pictures

(legend continued on next page)

Data S1, with the front panel shown in Fig. S7. To achieve wireless control of the camera using GigE drivers in LabVIEW, a virtual Ethernet connection was established by bridging the Wi-Fi adaptor and the Ethernet adaptor. A detailed procedure is given in Supporting Materials and Methods, Notes 2 and 3. To achieve good signal reception, we used a desktop PCI Express Network Adaptor (Intel 6050; Intel, Santa Clara, CA) with external antennas. To ensure the best data transmission, we activated the "resend lost packets" feature on the camera (specific parameters are reported in Table S2).

Sample and microsphere preparation

DNA constructs were prepared by hybridizing 123 oligonucleotides (Integrated DNA Technologies, Coralville, IA) to 7249-nt single-stranded M13mp18 DNA, as described in a previous work (12). The oligo hybridizing to the 3′ end of the M13 DNA contains double biotin on its 5′ end for immobilization to streptavidin-coated glass surface or the bead. The oligo hybridizing to the 5′ end of the M13 DNA extends beyond the M13, resulting in a 3′ single-stranded overhang (Fig. S8). Different constructs can be prepared by just varying this oligo hybridizing the 5′ end of M13 DNA. For shearing experiments in this study, the construct pairs that are immobilized to the glass slide and to the microspheres contain the 5′ hybridizing oligonucleotide that has a complementary sequence in the overhang region. The list of all oligos used is given in Table S3.

To immobilize the above prepared DNA constructs to streptavidin-coated microspheres (Dynabeads M-270, 2.8-μm diameter, catalog #65306; Thermo Fisher Scientific), we took 20 μL of streptavidin microspheres and washed thrice with 50 μL of 0.1% Tween 20 in phosphate-buffered saline (PBS). After the wash, the beads solution was brought to a 10 μL volume, and 10 μL of the DNA construct ($\sim$500 pM) was added to it and shaken in a vortexer at 1400 rpm for 30 min. The unbound DNA was removed by washing the beads thrice with 50 μL of 0.1% Tween 20 in PBS. The beads solution was brought to 40 μL volume.

Chamber preparation

The reaction chamber is prepared according to previous work (12). Briefly, the reaction chamber consists of an 18-mm and a 12-mm circular microscope glass slide (catalog #72230-01 and 72222-01; Electron Microscopy Sciences, Hatfield, PA) sandwiching two parallel strips of Kapton tape (www.kaptontape.com), creating a channel of $\sim$2 mm between the glass-slides. The glass chamber is assembled on top of a SM1A6-threaded adaptor (Thor Labs, Newton, NJ). Streptavidin (Amresco, Dallas, TX) was passively adsorbed to the surface by passing 10 μL of streptavidin (0.1 mg/mL) in 1$\times$ PBS. After 1 min of incubation, the chamber was washed thrice with 50 μL of PBS plus 0.1% Tween 20 to remove any unbound streptavidin. Next, 10 μL of DNA construct was passed through the channel and incubated for 5 min for the biotin-labeled DNA constructs to bind the streptavidin to the glass surface. The chamber was then washed with PBS plus 0.1% Tween 20 to remove unbound constructs. DNA-coated microspheres were passed into the chamber, and the chamber was sealed with vacuum grease, incubated for 2 min for the complementary strands to hybridize, then loaded into the CFM just before the experiment was performed.

Experimental protocol

To set up for an experiment, the camera must be plugged into the router, and the battery must be connected to power the CFM. Once these connections are made, the Wi-Fi signal from the router will appear in the network options on the computer. Once the connection from the router is established, the camera can be accessed from the LabVIEW program (Fig. S7). The run button on the LabVIEW toolbar activates streaming from the camera. The sealed chamber was screwed into the base of the lens tube (part# SM1L05; Thorlabs), and the lens tube was then screwed into the rest of the optical assembly until the beads were in focus. The CFM was then loaded into the centrifuge bucket, and the speed was controlled from the front panel of the centrifuge. The force generated on the tether is the centrifugal force experienced by the beads, $F = m\omega^2 r$, where m is the effective mass of the bead (actual mass-mass of buffer displaced), ω is the angular velocity, and r is the distance from the center of the rotor to the chamber (0.133 m). The effective mass of beads was determined to be 6.9×10^{-12} g for the Dynabeads M-270 (Thermo Fisher Scientific; www.thermofisher.com) by previous report (9) and 2.6×10^{-12} g for 5.2-μm polystyrene beads (catalog #SVP-50-5; Spherotech, Lake Forest, IL; www.spherotech.com). Mass calculation of the beads and the rpm used in the experiments are shown in Tables S4 and S5.

Data analysis

The data obtained from the CFM were analyzed using custom-written MATLAB (The MathWorks, Natick, MA) 2019 program. The program identifies beads using the inbuilt "imfindcircles" algorithm with a user override for nonspherical beads and dirt wrongly identified as beads. Once the beads are identified from the image at the start of the experiment, the software calculates the variance of the image intensity at the bead location for all the frames. When beads dissociate, it is indicated by the sharp drop in variance. Multiple drops in variance observed are due to the break in multiple-tethered beads, which are excluded from the analysis. The MATLAB code for this program is provided in Data S1. The data plots are constructed in OriginPro 2018, and fitting of data was done using inbuilt single exponential decay function, $y = y_0 + A \times \exp(-kt)$, where y is the fraction of tethers remaining at a given time t, y_0 is the y axis offset or the baseline, A is the fraction of tethers at the beginning of the experiment (typically 1), and k is the off rate for that particular force. The off rate for any given condition is determined by at least triplicate experiments in which individual k-values were determined separately; data were reported as the mean and standard deviation of the replicates.

RESULTS AND DISCUSSION

Instrument development

We had two main improvement goals in the development of our newest CFM: to establish real-time wireless control and streaming and to ensure an upgrade pathway for future CFM generations. Our previous CFM setup using the Intel Edison computer required running "blind," with images stored on limited onboard memory and later transmitted wirelessly for analysis, providing a frustrating user experience. Furthermore, the Edison computer required programming skills to implement changes, and its abrupt discontinuation by Intel made us realize how difficult simple upgrades could be. To solve these challenges, we implemented a Wi-Fi streaming strategy using an onboard router coupled with a

of CFMs belonging to various generations, starting from the prototype CFM to the fourth generation of CFM (current work), are shown. Pictures of CFMs developed outside the Wong/Halvorsen lab are not shown. (*d*) Pictures of the fourth-generation CFM from various angles are shown. (*e*) Table of properties comparing different versions of CFMs is given. The current version of CFM reported in this study retains the best features from all the generations. To see this figure in color, go online.

GigE vision camera. Both Wi-Fi and GigE vision follow standardized protocols that are routinely updated as technology progresses, providing a measure of future proofing for our CFM as wireless and camera technologies continue to improve. By using these standard communication protocols, we are also free to use any common programming language (including LabVIEW) for instrument control.

To implement this strategy, we started from the basic microscopy module developed previously (12) and substituted the USB camera from that design to a GigE camera. We next identified two different Wi-Fi routers that were small enough to fit within our microscope module inside a centrifuge bucket. The first was a commercial travel router (TP-Link AC750) with a theoretical bandwidth of 100 Mbps limited by the Ethernet port speed, and the second was an industrial grade OEM router (EmbedAir1000 from Acksys Communications and Systems, Villepreux, France) with a theoretical bandwidth of 557 Mbps limited by the wireless radio capabilities. We devised a networking scheme to establish a virtual Ethernet connection between the camera and the computer by connecting the camera to the router in access point mode and accessing the Wi-Fi signal from a desktop computer (Fig. 2, *a* and *b*). A step-by-step networking guide for both routers is provided in the Supporting Materials and Methods, Notes 2 and 3.

Once the basic connection scheme was established, we designed 3D-printed housings to hold the CFM components, including the new routers and support electronics. We also developed a wiring strategy to ensure the router and the camera have consistent power to remain connected for long periods in the centrifuge. With the router operating at 5 V and the GigE camera operating at 12–24 V, we used separate 5- and 12-V voltage step-up converters wired in series to a lithium-ion battery (the wiring diagram is in Figs. S2 and S4). We powered the LED light source separately from a coin cell battery. Using this configuration with a 2000-mAh battery resulted in a run time exceeding 2 h. We developed a LabVIEW program to control the camera, to display and store images, and to adjust relevant parameters such as frame rate, area of interest, and exposure time (Fig. S7; Data S1). Using this program, the captured images and the associated metadata, including timestamp, are transferred to the computer in real time, displayed on the screen, and stored on the computer hard disk for analysis.

Instrument validation and software development

For our first tests of the updated CFM, we assessed data transmission with each of the routers. We were able to consistently transmit data at a rate of 77.059 ± 0.002 Mbps with the commercial travel router and 454.3 ± 0.6 Mbps data with the industrial router (Fig. 2 *b*). These rates equate to 1.9 frames per second and 11.3 frames per second in full-frame mode for our 5-MP camera, and both represent ∼80% of the theoretical bandwidth of their respective routers. Faster frame rates can be obtained by reducing the frame sizes, but the maximal frame rates are often set by camera firmware. Next, we assessed transmission efficiency because wireless transmission can suffer from dropped packets. The GigE vision standard uses UDP protocol which has a higher data transfer rate than the common TCP protocol but does not guarantee packet delivery. We analyzed the data stream in different scenarios: 1) stationary CFM inside the centrifuge with an opened lid, 2) stationary CFM inside the centrifuge with a closed lid, and 3) spinning CFM with a closed lid at 500, 750, and 1000 rpm. We found that data transmission was not affected by closing the lid or spinning the device in the centrifuge, despite the thick walls of the centrifuge. We observed that both routers were able to transmit data with >99% reliability (Fig. 2 *c*), and packet loss appeared random.

Having validated the technical performance of our instrument's operation, we next developed a MATLAB postprocessing program for the analysis of single-molecule experiments from the CFM (Supporting File 8). For a model system, we considered a generic off-rate experiment in which microspheres tethered to a cover glass are exposed to force and dissociate over time (Fig. 3 *a*). We implemented this experiment using two biotinylated DNA handles that attach to either streptavidin-coated beads or cover glass and form tethers when complementary single-stranded overhangs bind to each other (Fig. 3 *a*). The DNA-tethered beads

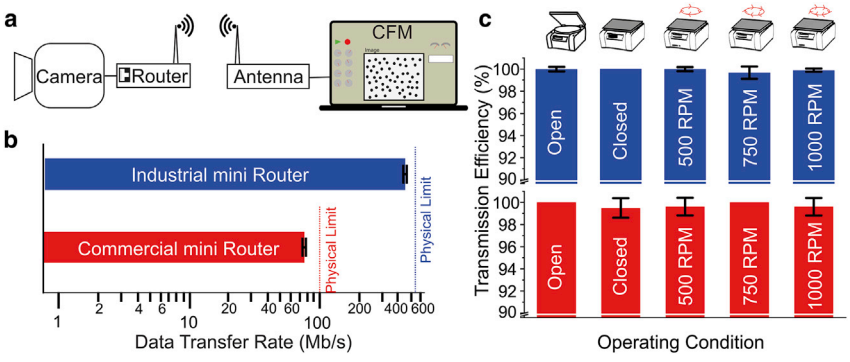

FIGURE 2 CFM networking strategy and streaming quality. (*a*) Schematic diagram showing wireless communication between the camera and the computer terminal is shown. (*b*) Measured data transfer rates using a commercial mini-router and an industrial grade OEM router are shown. (*c*) Quantified data transfer quality in various conditions using commercial mini-router (*red bars*) and industrial grade OEM router (*blue bars*) shows that the data transfer is >99% reliable. Very few images have lost data packets (which appear as dark pixels). Error bars report standard deviation from triplicate measurements. To see this figure in color, go online.

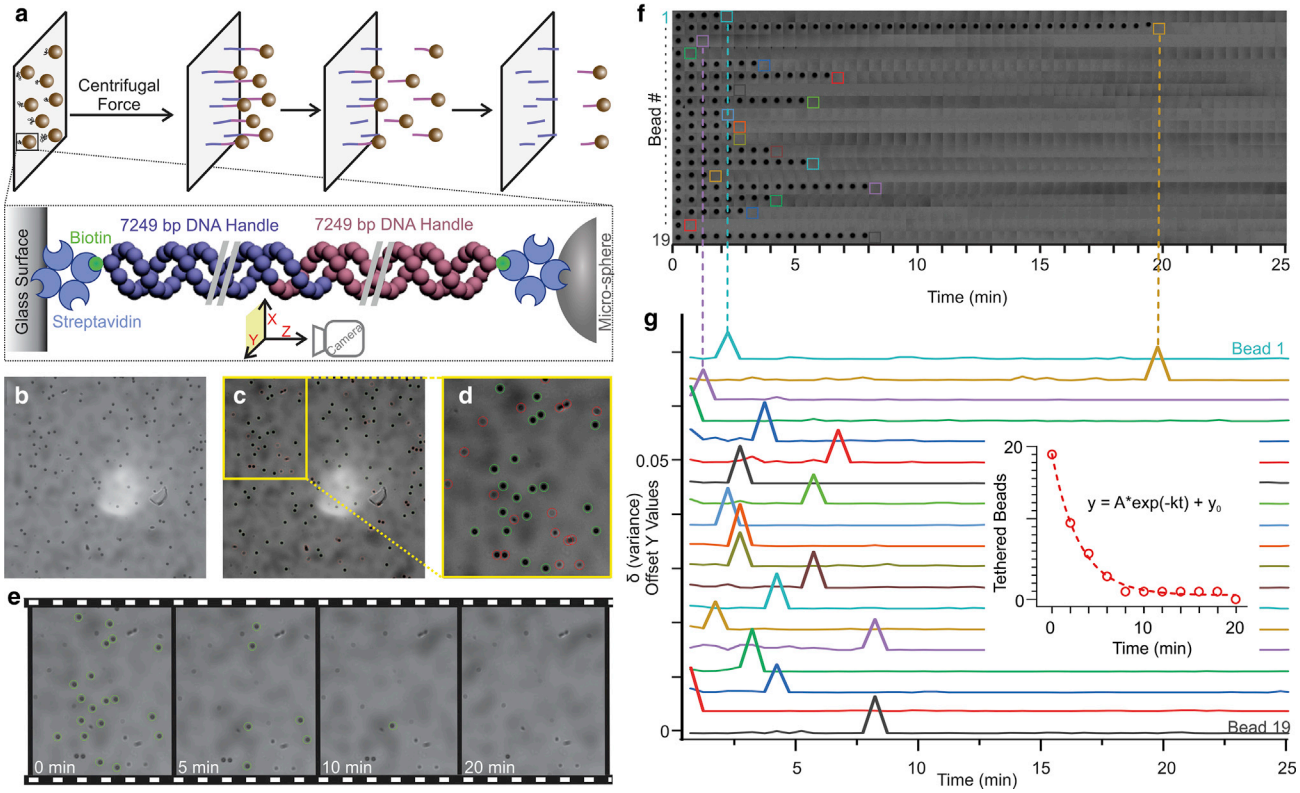

FIGURE 3 Experiment schematic and data analysis. (*a*) A schematic of single-molecule experiments is shown. The DNA handles with the sequence of interest are tagged to a glass side and a microbead. The hybridized DNA construct will unbind when force is exerted while spinning the CFM. (*b*) The image displays tethered beads under tension through the axis of view of the camera. (*c*) the image shows the bead selected through the MATLAB program for further analysis (*green*) and excluded beads (*red*). (*d*) Expanded view of a section of previous image is shown. (*e*) Images of area of interest at different time points are shown. It can be observed that the beads disappear as time progresses because of tether rupture under force. (*f*) Tracking of individual beads over time is shown. (*g*) Derivative plot of variance in the pixel intensity around the bead is shown. The variance will change when the bead dissociates from the surface, and this will appear in derivative plot as a peak; (*inset*) the cumulative decay plot of remaining tethers at a given point of time (*red circles*) is constructed from the derivative plot and kinetic parameters, such as off rates, at a particular force and can be obtained by fitting the cumulative with a single exponential decay function (*red line*). To see this figure in color, go online.

were observed in the CFM module and subjected to centrifugal force, with DNA shearing observed by bead detachment from the cover glass. The program was designed to identify tethered beads for analysis with a circle-finding algorithm and display color-coded circles on the images (Fig. 3, *b–d*). After identifying tethered beads, the software scanned all frames (Fig. 3 *e*) and constructed time traces of each bead to visually identify rupture frames (Fig. 3 *f*). For each bead in each frame, the image variance was calculated for a region of interest and was used to indicate rupture events (Fig. 3 *g*), which were plotted to display decay kinetics (Fig. 3 *g*, *inset*).

Single-molecule DNA shearing experiments with the CFM

To demonstrate the use of the updated CFM and software for single-molecule experiments, we performed DNA shearing experiments that showcase the dependence of force, length, and GC content in dissociation kinetics. DNA pulling experiments have long been a cornerstone of single-molecule experiments, both because of the ease of working with DNA as a tethering material and because of the many interesting biophysical properties of DNA (15,16). The mechanical stability of DNA junctions is of interest for natural biological processes such as genetic recombination (17) and for biotechnology applications such as DNA nanotechnology, in which DNA junctions are used as a sort of structural "glue" for nanomaterials (18). In the DNA nanotechnology field in particular, understanding the mechanical stability of short DNA duplexes has become increasingly important as DNA nanostructures increase in complexity to have mechanical linkages (19,20) and to support or apply forces (21). Here, we use our updated CFM to demonstrate how even minor differences in short duplexes can drastically affect their stability.

To perform the single-molecule experiments, we used the pair of cross-hybridizing biotinylated DNA handles described for Fig. 3 above and probed the kinetics with incorporation of different sequences in the short duplex (Fig. 4 *a*; Fig. S8). First, we investigated force-dependent

dissociation of a 7 bp interaction using force clamp experiments at 2–12 pN (Fig. 4 *b*). The off rates were determined by fitting the cumulative decay rates with a single exponential decay curve and ranged from 0.0034 ± 0.0009 to 0.0015 ± 0.0001 s^{-1}. We extrapolated the thermal off rate by fitting these data with the Bell-Evans model (Fig. 4 *c*; (22,23)), in which the force-dependent dissociation rate is described as k_{off} (f) = k_{off} exp (f/f_β), where k_{off} (f) is the off rate at the applied force f, k_{off} is the thermal off rate, and f_β is the characteristic force scale. Using this model, we found a thermal off rate k_{off} of 0.0013 ± 0.0001 s^{-1} and a force scale f_β of 13.0 ± 1.6 pN.

We also performed force clamp experiments at 4.5 ± 1.3 pN on DNA duplexes with lengths of 7, 8, and 9 bp to study the influence of DNA length and its thermodynamic stability (Fig. 4 *d*). We found the length-dependent off rates to be 0.0021 ± 0.0003, 0.00032 ± 0.00006, and 0.00027 ± 0.00006 s^{-1}, respectively, for 7, 8, and 9 bp (Fig. 4 *e*). This remarkable difference in the force-induced off rates suggests that this approach would also be sensitive to the GC content of the sequences, thereby opening up platforms for single-nucleotide polymorphism detection and force fingerprinting. To test the sensitivity of this approach, we designed an additional DNA construct based on the 7 bp interaction that replaced a single G-C pair with an A-T pair. We subjected both variants to a 12 ± 1.4-pN force clamp and measured the dissociation rates (Fig. 4 *f*) to be 0.0034 ± 0.0009 s^{-1} for the native duplex and 0.0145 ± 0.004 s^{-1} for the weakened duplex (Fig. 4 *g*). This indicates that the method is sensitive enough to distinguish a single-nucleotide variation in DNA fragments.

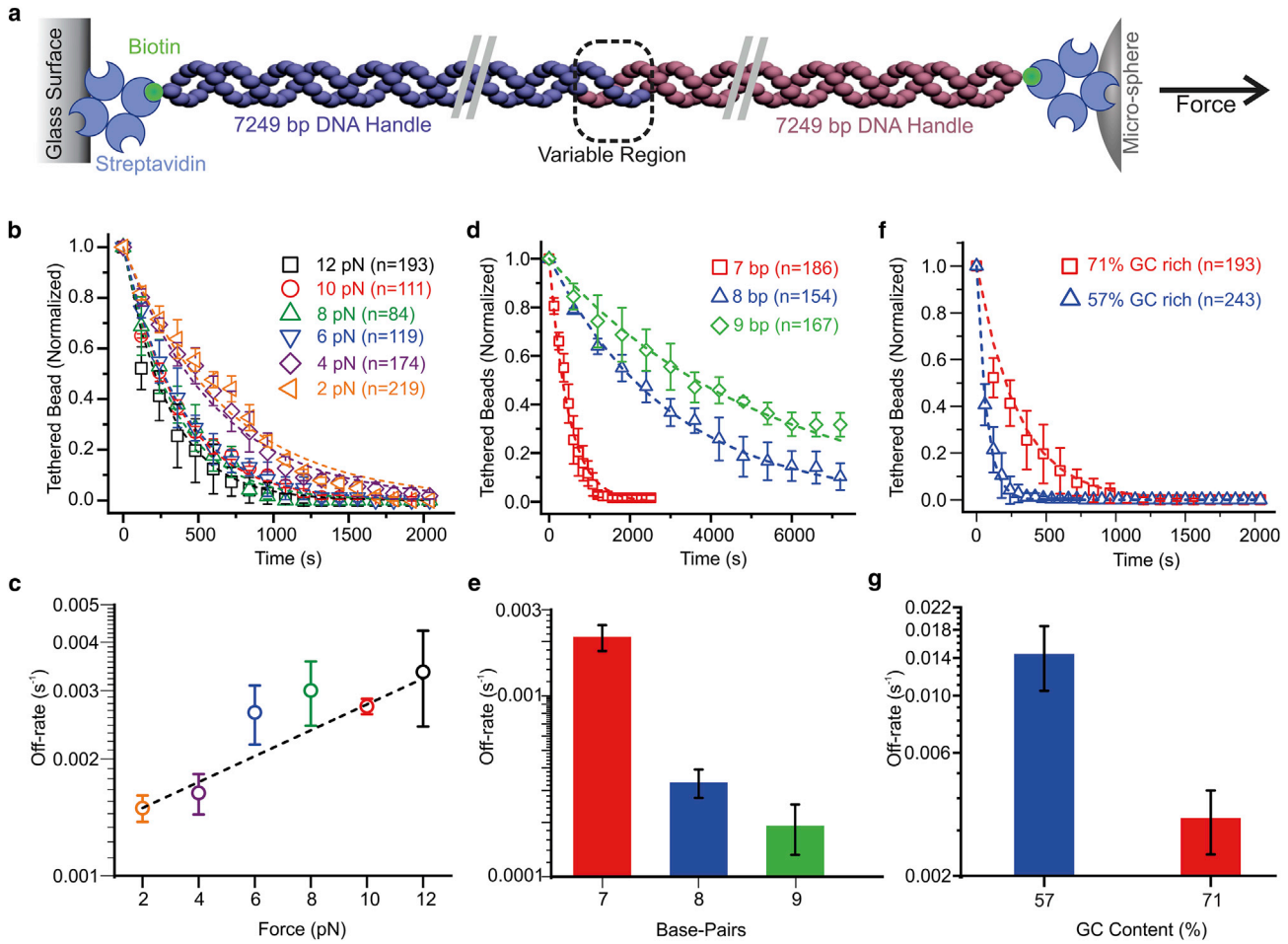

FIGURE 4 Single-molecule force clamp experiments with the CFM. (*a*) Schematics of an experiment in which force is applied to analyze the strength of DNA structures hybridized through complementary overhangs are shown. (*b*) Decay plot showing the effect of force (2–12 pN) for a 7 bp dissociation is shown. Off rates of the molecules can be determined by fitting the data with a single exponential decay (*dotted lines*). (*c*) Off rates determined at various forces can be used to determine thermal off rates by fitting the data with the Bell-Evans model. (*d*) The decay plot shows the dependency of length of the overhang on force-induced dissociation when held at a constant force of 4.5 pN. (*e*) Off rates of DNA shearing experiments containing 7–9 bp at 4.5 pN are shown. (*f*) Decay plot showing the dependency of GC content on DNA shearing when held at a constant force of 12 pN is shown. (*g*) Off rates are shown of DNA shearing experiments containing 7 bp at 12 pN, but with varied GC content by single GC to AT mutation. Error bars report standard deviation from triplicate experiments. To see this figure in color, go online.

A few studies, including our own work, have investigated forced dissociation of DNA duplexes in a shearing mode, but very little has been done on short (<10 bp) duplexes. AFM pulling experiments by Strunz et al. on duplexes of 10–30 bp extrapolated thermal off rates varying by many orders of magnitude, from $\sim 10^{-12}$ s^{-1} for 30 bp to $\sim 10^{-2}$ s^{-1} for 10 bp to ~ 0.3 s^{-1} for a 7 bp duplex (predicted) (24). These off rates are much faster than those that we have measured here and in our previous work (12), likely because of a combination of several effects, including extrapolation far from equilibrium AFM measurements as well as differences in the molecular construct. In our previous CFM work, we measured a 7 bp duplex in a similar setup and found dissociation rates that were faster but the same order of magnitude as those measured here, which we attribute to a difference in base-stacking interactions between the two molecular constructs. As we have seen from this work, even a small change in duplex design, such as a single-nucleotide variation, can cause a large difference in the force-dependent off rate.

Outlook for the CFM

The CFM sits within a landscape of other single-molecule approaches, so it is instructive to discuss the benefits and detriments of the CFM for potential users. Chief among the benefits are the high throughput due to multiplexing, low cost, and low barrier to entry for new users. In this work, we expand on the ease of use and further lower barriers to entry with detailed designs and software. Still, there are many challenges that remain for CFM development, including rapid changes in force, integration of flow, accessing millisecond and submillisecond timescales, nanometer-level axial tracking, and real-time focus adjustment. Several of these have been addressed individually in other works (e.g., nanometer-level tracking (10,14) and real-time focus adjustment (9)) but have not been brought all together as is now common for other techniques such as optical tweezers.

Considering the strengths and weaknesses of the CFM, we outline here a few types of experiments in which we think the approach can really excel:

1) Pulling experiments that result in rupture or a large (>100 nm) length change. These types of experiments (as demonstrated in this study) are relatively easy to set up and to analyze and benefit from the multiplexing of the CFM to get data in a short time.
2) Near-equilibrium experiments with long timescales (minutes to hours). The CFM can stably hold forces indefinitely and is thus perfectly suited for long timescale experiments. Multiplexing becomes especially compelling here. For example, collecting 1000 statistics of an hour-long dissociation could be done in a day on CFM and take many months on optical tweezers.
3) Force-dependent enzyme or molecular motor activity. For some studies involving enzyme or motors, activity may start upon building the sample chamber. Some extreme cases in optical tweezer experiments collected only one or a few data points per sample chamber (25,26), which could be greatly enhanced with multiplexing, as has been demonstrated for collagen proteolysis (13).
4) Analysis of molecular heterogeneity. CFM multiplexing opens new opportunities to study heterogeneity and to pull on an array of molecules repeatedly to track both variations between and within individual molecules in a population (10).
5) Teaching experiments or experiments involving undergraduates. The CFM is particularly friendly for undergraduates and biophysicists in training. Several undergraduates in our lab have operated it and successfully collected data, and a recent study from another lab even developed a student-focused CFM (27).

To summarize our developments here, we have unveiled a next-generation CFM that is completely plug-and-play with high-bandwidth live streaming over Wi-Fi. This instrument is, to our knowledge, the first CFM that offers similar performance to the fiber-optic-wired CFMs (9,10), but with the convenience and simplicity of a plug-and-play module (12). Also, our design considers future upgrades and ease of programming, opting for commercially available Wi-Fi components that are interchangeable and have standardized protocols. These design changes are centered around the user experience and making single-molecule experiments easier to perform. In that regard, the CFM is uniquely well suited among single-molecule techniques and can even be used by undergraduate students and researchers without a technical biophysics training.

As with previous builds, the CFM has a low cost compared with other single-molecule setups such as optical tweezers and AFM. The as-built CFM module in this study has a material cost of ~$2200, making it an affordable piece of equipment for individual labs (Table S1). Nearly 75% of the cost comes from the camera and the objective, providing a reasonable opportunity to lower costs to ~$1000 with alternative components. The centrifuge constitutes an additional cost, but most labs already have access to a benchtop centrifuge that can be used. We previously showed that 3D-printed adapters can be used to accommodate two other common centrifuge models that use larger bucket sizes (28). In the Supporting Materials and Methods and Data S1, we have provided all the details necessary to reconstruct the CFM instrument, including 3D models, parts lists, and step-by-step protocols.

Since the initial development of the CFM, there have been several other techniques that were developed to provide multiplexed single-molecule experimentation. There have been significant advances in multiplexed magnetic tweezers (29–31), as well as development of new technologies such as acoustic force spectroscopy (32) and optical pushing (33). These methods have helped expand the field,

especially with the commercialization of acoustic force spectroscopy, but we still believe that the CFM offers some distinct features for ease of use, low cost, and broad and calibration-free force range. With this current development, we further advance the state of the art in CFM design and make it easier than ever to build and use.

SUPPORTING MATERIAL

Supporting Material can be found online at https://doi.org/10.1016/j.bpj.2020.10.017.

AUTHOR CONTRIBUTIONS

The concept was initially conceived by K.H. Networking strategies were developed by J.A.P. and A.H. 3D designs for housing were developed by A.H. and L.Z. Experiments were designed by J.A.P. and were carried out by J.A.P. and A.H. Programs were developed by J.A.P. and K.H. All authors participated in data analysis, critical discussions, and writing of the manuscript.

ACKNOWLEDGMENTS

We thank Dr. Tony Hoang for technical help and suggestions, the University of Albany Research Information Technology team for help with networking, and Drs. Wesley Wong, Darren Yang, and Arun Richard Chandrasekaran for discussions on the project, for critical suggestions, and for edits of the manuscript. The corresponding author (K.H.) has patents and patent applications on the CFM instrument and use. Not-for-profit use of the CFM is not prevented by these patents.

Research reported in this publication was supported by the National Institutes of Health through the National Institute of General Medical Sciences under award R35GM124720 to K.H.

REFERENCES

1. Ritort, F. 2006. Single-molecule experiments in biological physics: methods and applications. *J. Phys. Condens. Matter.* 18:R531–R583.
2. Deniz, A. A., S. Mukhopadhyay, and E. A. Lemke. 2008. Single-molecule biophysics: at the interface of biology, physics and chemistry. *J. R. Soc. Interface.* 5:15–45.
3. Zlatanova, J., and K. van Holde. 2006. Single-molecule biology: what is it and how does it work? *Mol. Cell.* 24:317–329.
4. Nathwani, B., W. M. Shih, and W. P. Wong. 2018. Force spectroscopy and beyond: innovations and opportunities. *Biophys. J.* 115:2279–2285.
5. Gebhardt, J. C. M., T. Bornschlögl, and M. Rief. 2010. Full distance-resolved folding energy landscape of one single protein molecule. *Proc. Natl. Acad. Sci. USA.* 107:2013–2018.
6. Dietz, H., and M. Rief. 2004. Exploring the energy landscape of GFP by single-molecule mechanical experiments. *Proc. Natl. Acad. Sci. USA.* 101:16192–16197.
7. Block, S. M., L. S. Goldstein, and B. J. Schnapp. 1990. Bead movement by single kinesin molecules studied with optical tweezers. *Nature.* 348:348–352.
8. Davenport, R. J., G. J. Wuite, …, C. Bustamante. 2000. Single-molecule study of transcriptional pausing and arrest by *E. coli* RNA polymerase. *Science.* 287:2497–2500.
9. Halvorsen, K., and W. P. Wong. 2010. Massively parallel single-molecule manipulation using centrifugal force. *Biophys. J.* 98:L53–L55.
10. Yang, D., A. Ward, …, W. P. Wong. 2016. Multiplexed single-molecule force spectroscopy using a centrifuge. *Nat. Commun.* 7:11026.
11. Yang, D., and W. P. Wong. 2018. Repurposing a benchtop centrifuge for high-throughput single-molecule force spectroscopy. *In* Single Molecule Analysis: Methods and Protocols. E. J. G. Peterman, ed. Springer, pp. 353–366.
12. Hoang, T., D. S. Patel, and K. Halvorsen. 2016. A wireless centrifuge force microscope (CFM) enables multiplexed single-molecule experiments in a commercial centrifuge. *Rev. Sci. Instrum.* 87:083705.
13. Kirkness, M. W. H., and N. R. Forde. 2018. Single-molecule assay for proteolytic susceptibility: force-induced collagen destabilization. *Biophys. J.* 114:570–576.
14. Kou, L., L. Jin, …, X. Hu. 2019. Real-time parallel 3D multiple particle tracking with single molecule centrifugal force microscopy. *J. Microsc.* 273:178–188.
15. Bustamante, C., Z. Bryant, and S. B. Smith. 2003. Ten years of tension: single-molecule DNA mechanics. *Nature.* 421:423–427.
16. Bustamante, C., S. B. Smith, …, D. Smith. 2000. Single-molecule studies of DNA mechanics. *Curr. Opin. Struct. Biol.* 10:279–285.
17. Schwacha, A., and N. Kleckner. 1995. Identification of double Holliday junctions as intermediates in meiotic recombination. *Cell.* 83:783–791.
18. Jones, M. R., N. C. Seeman, and C. A. Mirkin. 2015. Nanomaterials. Programmable materials and the nature of the DNA bond. *Science.* 347:1260901.
19. Marras, A. E., L. Zhou, …, C. E. Castro. 2015. Programmable motion of DNA origami mechanisms. *Proc. Natl. Acad. Sci. USA.* 112:713–718.
20. Zhou, L., A. E. Marras, …, H.-J. Su. 2018. Paper origami-inspired design and actuation of DNA nanomachines with complex motions. *Small.* 14:e1802580.
21. Nickels, P. C., B. Wünsch, …, T. Liedl. 2016. Molecular force spectroscopy with a DNA origami-based nanoscopic force clamp. *Science.* 354:305–307.
22. Bell, G. I. 1978. Models for the specific adhesion of cells to cells. *Science.* 200:618–627.
23. Evans, E., and K. Ritchie. 1997. Dynamic strength of molecular adhesion bonds. *Biophys. J.* 72:1541–1555.
24. Strunz, T., K. Oroszlan, …, H. J. Güntherodt. 1999. Dynamic force spectroscopy of single DNA molecules. *Proc. Natl. Acad. Sci. USA.* 96:11277–11282.
25. Zhang, X., K. Halvorsen, …, T. A. Springer. 2009. Mechanoenzymatic cleavage of the ultralarge vascular protein von Willebrand factor. *Science.* 324:1330–1334.
26. Neuman, K. C., E. A. Abbondanzieri, …, S. M. Block. 2003. Ubiquitous transcriptional pausing is independent of RNA polymerase backtracking. *Cell.* 115:437–447.
27. Tompkins, K. J., N. Venkatesh, …, W. R. Gordon. 2020. Student-focused development of a next-generation centrifuge force microscope. *bioRxiv* https://doi.org/10.1101/2020.08.30.274373.
28. Hoang, T., N. Moskwa, and K. Halvorsen. 2018. A 'smart' tube holder enables real-time sample monitoring in a standard lab centrifuge. *PLoS One.* 13:e0195907.
29. De Vlaminck, I., and C. Dekker. 2012. Recent advances in magnetic tweezers. *Annu. Rev. Biophys.* 41:453–472.
30. De Vlaminck, I., T. Henighan, …, C. Dekker. 2012. Magnetic forces and DNA mechanics in multiplexed magnetic tweezers. *PLoS One.* 7:e41432.
31. Agarwal, R., and K. E. Duderstadt. 2020. Multiplex flow magnetic tweezers reveal rare enzymatic events with single molecule precision. *Nat. Commun.* 11:4714.
32. Sitters, G., D. Kamsma, …, G. J. L. Wuite. 2015. Acoustic force spectroscopy. *Nat. Methods.* 12:47–50.
33. Sitters, G., N. Laurens, …, G. J. L. Wuite. 2016. Optical pushing: a tool for parallelized biomolecule manipulation. *Biophys. J.* 110:44–50.